International Journal of Non-Linear Mechanics 77 (2015) 364–375

Contents lists available at ScienceDirect

International Journal of Non-Linear Mechanics

journal homepage: www.elsevier.com/locate/nlm

Primary resonance of a beam-rigid body microgyroscope

S.A.M. Lajimi *, G.R. Heppler, E.M. Abdel-Rahman

Systems Design Engineering, University of Waterloo, Canada N2L 3G1

ARTICLE INFO

Article history:
Received 24 January 2015
Received in revised form
28 May 2015
Accepted 1 July 2015
Available online 15 July 2015

Keywords:
Gyroscope
Method of multiple scales
Shooting method
Non-linear dynamics
Frequency-modulation
Entrainment

ABSTRACT

We present the non-linear dynamical features of a beam-rigid-body microgyroscope operating under the electrostatic force. A comprehensive system of discretized governing equations is solved using the method of multiple scales and the shooting method. For an amplitude-modulation gyro, the effects of the quality factor, AC voltage, and the rotation rate on the response are investigated and the fold-bifurcation points are identified. A frequency-modulation gyro is examined and in addition to the bifurcation points, the entrainment region is identified. The effects of a positive and a negative internal detuning parameter on the frequency-response of a frequency-modulation gyro are investigated.

1. Introduction

Capacitive transducers constitute the majority of sensing methods in micro-electro-mechanical systems (MEMS) requiring electrostatic actuation of the microstructure [1]. For the commonly used variable-gap transducers, the force is proportional to the reciprocal of the gap distance between the pairs of the electrodes squared. The moving electrode is obtained by etching a beam-like structure on a silicon layer and the fixed electrode is formed either beside or beneath the beam. The reciprocal quadratic non-linearity causes the system to show instability and bifurcation in different types of MEMS [2,3].

Multi-port transducers such as gyroscopes introduce additional complexities into the system because of the inherent difficulties of their mechanics. A gyroscopic system such as a beam rotating about an axis perpendicular to its neutral axis shows complex non-linear dynamical features in free vibration [4]. There are a few studies concerning the non-linear vibration of microgyroscopes. Braghin et al. [5] considered a tuning fork MEMS gyroscope, a variable-area capacitive transducer, approximated the system with a lumped-mass model, and studied the system using the Galerkin–Urabe method. They showed that under the comb-drive electrostatic actuation of their system a hardening behaviour appears.

Including the electrostatic non-linearity into Esmaeili et al.'s gyro model [6], Ghommem et al. [7] reduced the order of simplified equations of a perfectly symmetric beam-based (amplitude-modulation) gyro and briefly studied its non-linear vibration ignoring the effect of frequency mismatch. Similarly, Lajimi [8] used a continuation tool to briefly study the non-linear dynamics of a symmetric beam-based gyro neglecting the effect of internal detuning parameter.

Leland [9] derived the slow model of the system using the method of averaging for a single-mass oscillator gyroscope. By taking the Laplace transform of his linear system of equations, Leland arrived at a closed form relation for computing the noise equivalent rotation rate for the gyroscope. Later Leland [10] used the averaged system to derive an adaptive control law to compensate for the errors associated with quadrature coupling and damping. Oropeza et al. [11] studied a parametrically excited MEMS gyroscope and showed its advantages in offering high sensitivity and bandwidth.

In the following, we offer a different approach and obtain the slow system which could be used for mechanical-thermal noise analysis of the gyroscope and deriving proper control laws to compensate for the errors in the system. Properly characterizing the non-linear dynamics of a rotation rate sensor (a microgyroscope) is necessary for the design optimization as well. To this end, the effect of frequency mismatch is taken into consideration by introducing an internal detuning parameter into the equations of motion. Here we consider a

* Corresponding author.
E-mail addresses: samousav@uwaterloo.ca, samirm@sfu.ca (S.A.M. Lajimi).

http://dx.doi.org/10.1016/j.ijnonlinmec.2015.07.002
0020-7462/© 2015 Published by Elsevier Ltd.

microgyroscope rotating about its longitudinal axis carrying a large end-mass, comprised a rigid-body, affecting the system dynamics. We include the effects of the Coriolis force and the centrifugal force to account for the stiffening of the beam.

We investigate the discretized system of equations using the method of multiple scales and the shooting method. To this end, separating the modal coordinates into their static and dynamic components, we solve the dynamic equations using the method of multiple scales. The equilibrium equations of the "slow" system are obtained and solved using numerical methods. We characterize the non-linear dynamics of both amplitude-modulation and frequency-modulation gyros by introducing internal and external detuning parameters into the modulation equations. We identify a synchronization region in the frequency-response curves of the mismatched gyro using both perturbation method and shooting method.

2. Mathematical methods

The schematic of the sensor is provided in Fig. 1. A feasible inexpensive fabrication process requires one to have a uniform thickness along the length of the micro-structure including the beam and the end-mass. To reduce the effect of squeeze-film damping which increases with area [12,13], we consider etching two holes in the end-mass.

2.1. Equations of motion

Employing the extended Hamilton's principle, the governing equations of motion are obtained as [14,15]

$$EI_{\eta\eta}\, w'''' + m\,\ddot{w} + 2\,m\,\Omega\,\dot{v} + m\,\dot{\Omega}\,v - m\,\Omega^2 w + c_w\,\dot{w} - J_{B\eta\eta}\,\Omega^2 w'' - J_{B\eta\eta}\,\dot{\Omega}\,v'' - J_{B\eta\eta}\,\ddot{w}'' = 0, \tag{1}$$

$$EI_{\zeta\zeta}\, v'''' + m\,\ddot{v} - 2\,m\,\Omega\,\dot{w} - m\,\dot{\Omega}\,w - m\,\Omega^2\,v + c_v\,\dot{v} - J_{B\zeta\zeta}\,\Omega^2\,v'' - J_{B\eta\eta}\,\dot{\Omega}\,w'' - J_{B\zeta\zeta}\,\ddot{v}'' = 0, \tag{2}$$

and the boundary conditions are given by

$$w=0, \quad w'=0, \quad v=0, \quad v'=0 \quad \text{at } \ell=0, \tag{3}$$

and at $\ell = L$ by

$$\begin{aligned} &EI_{\eta\eta}\, w'' - M\,e\Big(\Omega^2(w+e\,w') - \dot{\Omega}(v+e\,v') - 2\,\Omega(\dot{v}+e\,\dot{v}') - (\ddot{w}+e\ddot{w}')\Big) + J_{M\eta\eta}\Big(\dot{\Omega}v' + \Omega\dot{v}' + \ddot{w}'\Big) \\ &+ J_{M\xi\xi}\Big(\Omega^2\,w' - \Omega\,\dot{v}'\Big) - J_{M\zeta\zeta}\Big(\Omega^2\,w' - \Omega\,\dot{v}'\Big) = \frac{\epsilon\,e_w\,A_w\,V_w^2}{2(g_w - w - e\,w')^2}, \end{aligned} \tag{4}$$

$$\begin{aligned} &EI_{\zeta\zeta}\, v'' - M\,e\Big(\Omega^2(v+e\,v') + \dot{\Omega}(w+e\,w') + 2\,\Omega(\dot{w}+e\,\dot{w}') - (\ddot{v}+e\ddot{v}')\Big) + J_{M\zeta\zeta}\Big(\ddot{v}' - \dot{\Omega}w' - \Omega\,\dot{w}'\Big) \\ &- J_{M\eta\eta}\Big(\Omega^2\,v' + \Omega\,\dot{w}'\Big) + J_{M\xi\xi}\Big(\Omega^2\,v' + \Omega\,\dot{w}' + \dot{\Omega}w'\Big) = \frac{\epsilon\,e\,A_v(v(L,t) + e_v\,v'(L,t))V_v^2}{\Big(g_v^2 - (v(L,t) + e\,v'(L,t))^2\Big)^2}, \end{aligned} \tag{5}$$

$$\begin{aligned} &EI_{\eta\eta}\, w''' + M\Big(\Omega^2(w+ew') - \dot{\Omega}(v+ev') - 2\Omega(\dot{v}+e\,\dot{v}') \\ &- (\ddot{w}+e\ddot{w}')\Big) - J_{B\eta\eta}\Big(\dot{\Omega}v' + \Omega^2 w' + \ddot{w}'\Big) = -\frac{\epsilon\,A_w\,V_w^2}{2(g_w - w - e\,w')^2}, \end{aligned} \tag{6}$$

$$EI_{\zeta\zeta}\, v''' + M\Big(\Omega^2(v+ev') + \dot{\Omega}(w+ew') + 2\Omega(\dot{w}+e\,\dot{w}')$$

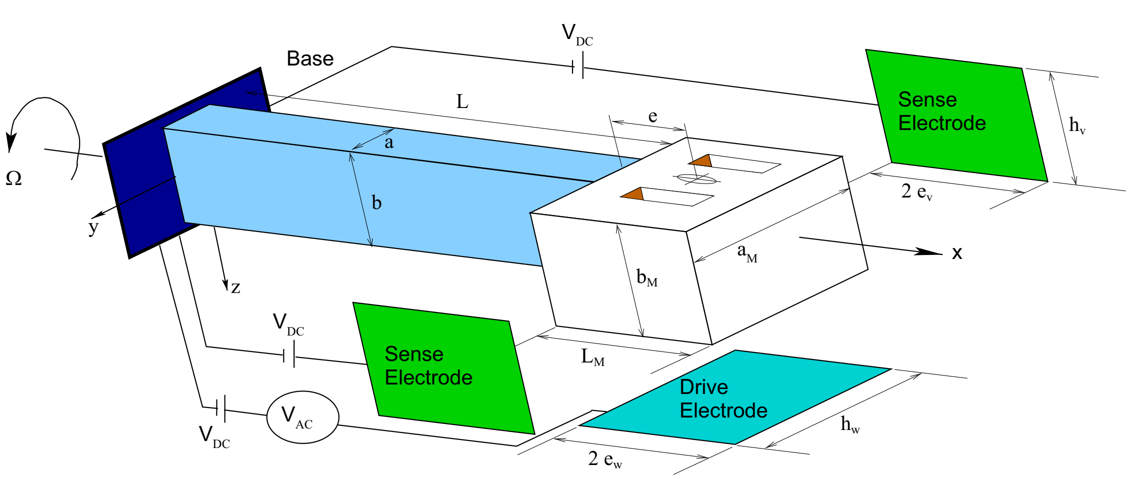

Fig. 1. Schematic of the beam-rigid-body microgyroscope (MEMS Gyroscope). The figure is not drawn to scale.